



*Image processing,
Computer aided diagnosis,
Measurements of brain ventricular system*

Arkadiusz GERTYCH¹, Alexis WONG^{2,1}

SEGMENTATION OF LATERAL VENTRICLES FOR MONITORING OF PATIENT'S STATUS WITH NORMAL PRESSURE HYDROCEPHALUS

Assessment of brain ventricular size is an important factor in both the diagnosis and post-surgical evaluation of patients that may respond to shunt therapy for suspected cases of normal pressure hydrocephalus (NPH). A lack of currently accepted and standardized criteria for diagnosing and classifying NPH patients precludes objective identification. Currently, three clinical soft qualifiers are used to categorize the likelihood of NPH: probable, possible, and unlikely. These are assessed by clinical symptoms, patient history, and results of brain imaging supported by manual measurements performed by a neuroradiologist. In this study we propose to enhance existing clinical characteristic of a diagnosed patient by incorporating automatic segmentation and calculation of the volume of the lateral ventricles. Methodology presented in this paper is based on volume data analysis including: location of interhemispheric line location, fuzzy c-means segmentation, morphological operations and 3D connectivity analysis in segmented image data. This approach was developed and tested on T1/T2 brain MRI studies of 40 control cases and 7 NPH cases with 5mm cross sections showing acceptable accuracy.

1. INTRODUCTION

Classification and measurements of normal and abnormal intracranial compartments are the goals of segmentation procedures applied to quantitative evaluation of brain MR studies with specific regard to chronic degenerative disorders requiring serial controls over long period of time. Alzheimer disease (AD), normal pressure hydrocephalus (NPH), and multiple sclerosis (MS) serve as examples. NPH (fig.1) is a chronic accumulation of excess cerebrospinal fluid (CSF) within the ventricles (four inner, fluid-filled chambers) of the brain which causes the ventricles to dilate, stretching parenchymal (brain) tissue and resulting in a variety of clinical symptoms. NPH typically affects adults aged over 55, causing the classic triad of ataxia, urinary incontinence, and dementia. The symptoms of NPH appear to progress over time with a variable but often inevitable deterioration to disability or a critical loss of function. Although the exact incidence of NPH disorder in the American population is unknown, it is estimated that 375,000 people or 5% of the US population with dementia (including Alzheimer disease) may have NPH. Currently there is lack of accepted and standardized criteria for the diagnosis of NPH. Current diagnosis is based on

¹ University of Southern California, Keck School of Medicine, Image Processing and Informatics Laboratory,
4676 Admiralty Way, Suite 601, Marina Del Rey, CA 90292

² University of Southern California, Department of Radiology, 1975 Zonal Avenue KAM 500, Los Angeles, CA 90089

convergent evidence from clinical history, examination and brain imaging [1], [2]. Brain imaging involves CT, MR or radionuclide cisternography to affirm ventriculomegaly and/or abnormal CSF flow. Three soft qualifiers: probable, possible, and unlikely are utilized in the current classification scheme of NPH. Shunt placement (surgical decompression) is the treatment of choice for the select group patients determined to likely benefit from invasive therapy. Initial evaluation of surgical candidacy is very important. In 70-75% of cases of qualifying patients subjected to shunt surgery, there is significant clinical improvement following intervention [2], while in the remaining cases there is no improvement. Selection of shunt candidacy is presently supported by patient history and 2D/3D manual measurements in MR/CT studies. Among these measurements, the volume of the lateral ventricles plays an important role. This finding is also used in the assessment of shunt patency for management of patients who failed to improve or are clinically deteriorating. Routine clinical protocol for brain imaging of NPH patients sometimes includes cross-sections thicker than 3mm with gaps between cross-sections. Some of existing methods [3-5] of segmentation of brain ventricular system (VS) described in the literature are adjusted to analyze image data of 3mm slice thickness and smaller often with no gaps.

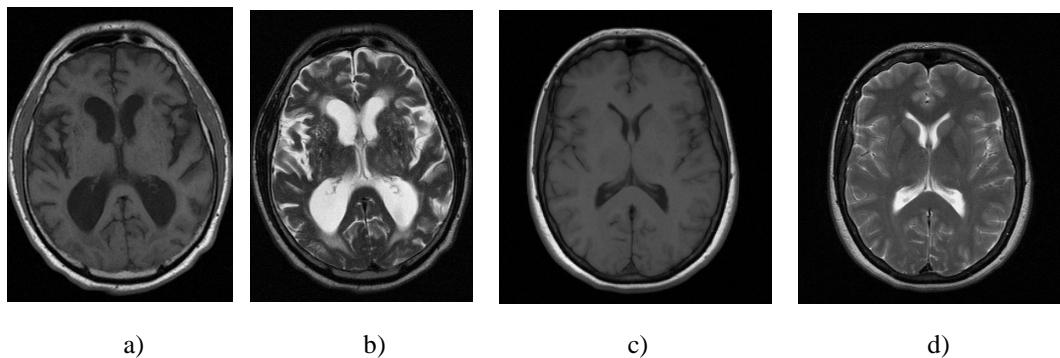


Figure 1. Examples of ventricular system in MR imaging: a), b) T1/T2 images of dilated ventricular system of 68 year old male NPH patient, c), d) T1/T2 images of ventricular system within normal limits of 54 year old female.

In this paper an automated approach to lateral ventricles segmentation from T1/T2 head MR studies is presented. Head mask and interhemispheric lines location are followed by a 3D fuzzy c-means (FCM) segmentation of a 3D lateral ventricles region from T1 images. Segmented CSF spaces were subjected to a morphological analysis preserving connected components in 3D space and yielding lateral ventricles LV volume. The method was developed and tested based on clinical image data of NPH and control patients.

2. MATERIALS AND METHODS

2.1. IMAGE DATA

Currently, seven MRI cases of patients with confirmed NPH and a control group of 40 normal MRI cases of patients aged 45 to 80 years have been collected. The data was randomly split into training (20 controls, 3 NPH) and testing (other cases) parts. All studies contain T1/T2 weighted axial MR sequences with matrices of 256x256 (T1) or 512x512 (T2) and 12 bits/pixel resolution acquired by a 1.5T MR Scanner. Thicknesses of cross-sections are 5mm with 1.75mm or 2mm gaps

respectively. Pixel size of T1 images is of 0.89mm x 0.89mm and T2 is of 0.449mm x 0.449mm respectively. Image data have been acquired at USC University Hospital, and USC Health Consultation Center II in Los Angeles.

2.2. METHOD

2.2.1 HEAD MASK LOCATION

An overview of the methodology of volume image data analysis is depicted in the Figure 2. At the preliminary stage, series size standardization of a study is performed. In the data repository, T1 and T2 acquisitions of the same study have different spatial resolutions; hence the larger images (mostly T2) are resized to fit the size of T1 acquisition data. Image analysis starts with background removal procedure. It can be done by histogram thresholding of the entire volume data (fig.3a) [10]. This procedure yields a 3D head mask. The mask is refined by a 2D binary erosion procedure to suppress ring artifacts and to partially remove skin objects. After this step a refined head mask is obtained.

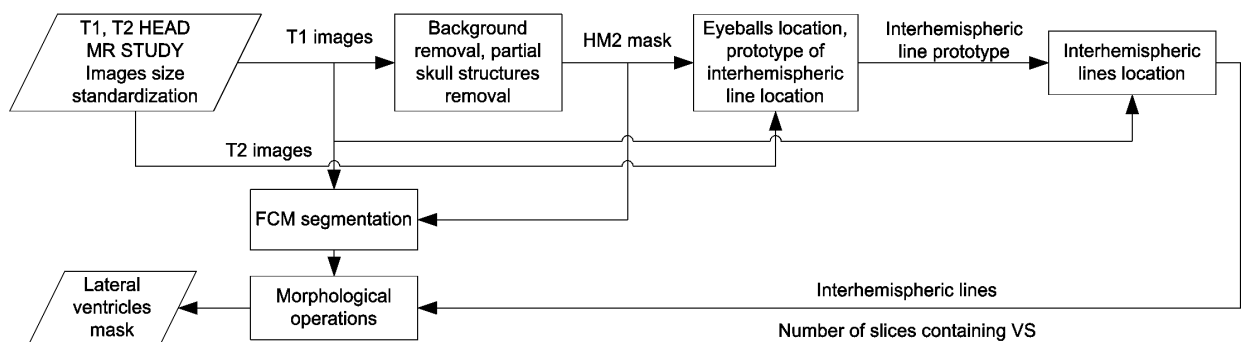


Figure 2. Lateral ventricles location in head MR study workflow.

Next, volume data of T1 acquisition delimited by the refined head mask is subjected to bony removal procedure. In a typical histogram of T1 volume data (fig. 3b) four components can be distinguished.

In this case it is assumed that analyzed series consist of cerebrospinal fluid (CSF), white matter (WM), gray matter (GM) and bony structure (BS) objects. Separation of these anatomical structures is often hampered by the presence of field intensity inhomogeneity artifacts, diverse skull structure signal characteristics and differences in appearance between normal and pathological tissues. Statistics of T1 volume data is modeled by a 4-class Gaussian mixture data model. Model components are calculated by means of expectation-maximization algorithm [11]. This approach yields mean values and standard deviations (N_{str}, σ_{str}) when str is referred to the tissue model (CSF, WM, GM, BS) (fig. 3b). One can see that the last peak of the histogram representing pixels of bony structures can be distinguished from the rest of the histogram model. In order to separate this peak, a thresholding value of $T_{BS} = N_{BS} - 2\sigma_{BS}$ is set and a binary head mask (HM2) with suppressed bony structure is obtained. HM2 mask is used in next steps of the methodology described in this paper.

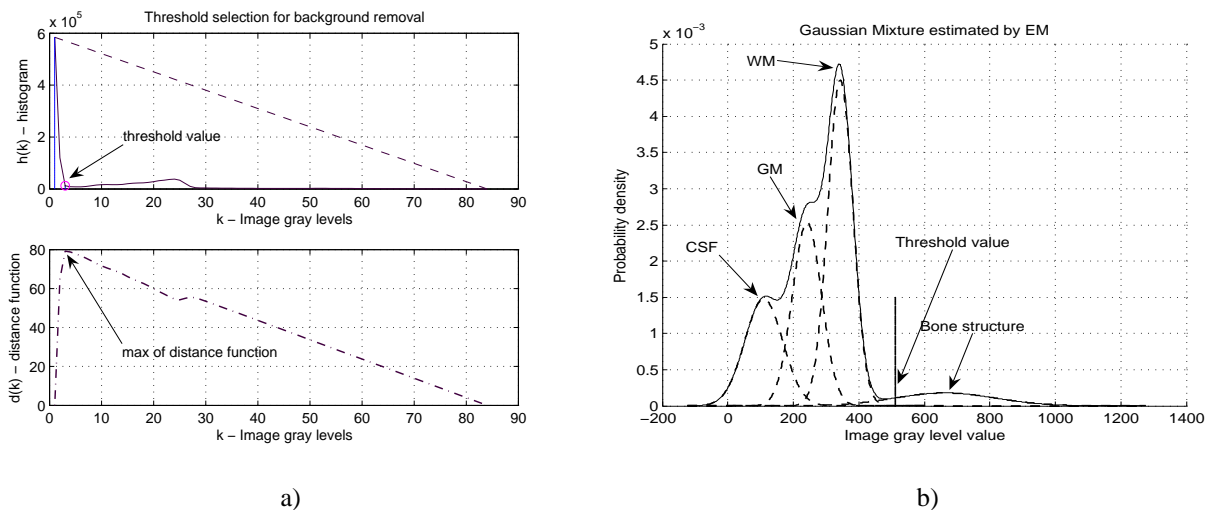


Figure 3. Histograms of T1 volume data: a) removal of background by [10], b) modeled by EM method [11].

2.2.2 INTERHEMISPHERIC LINES LOCATION

Various tasks involving segmentation of intracranial structures like location of brain landmarks, brain registration and calculation of intracranial structure volume can be simplified by location of midsagittal lines and the midsagittal plane [12-13]. It can be done by detection of series of lines along the interhemispheric fissure in axial cross-section data set. In [12-13] robust approaches to this problem have been described. They are based on local symmetry and outlier removal of human cerebrum in MR images. In our work an automated approach based on 2D T1 data analysis with localization of the rough prototype of an interhemispheric fissure line (PIL) in T2 series is used. In this paper it is assumed that IL can be found based on symmetry of eyeballs in T2 images and symmetry of borders of intracranial structures in T1 images (fig. 2). Similarly to other fluid containing structures (fig. 1), the eyeballs in T2 MR images appear as hyper intense objects and thus they appear as very last component in the histogram of T2 data [8]. In order to localize the eyeballs the T2 volume data is subjected to 3-class fuzzy c-means procedure [9]. Next segmented 3D volume is labeled by a labeling routine [14] and detection of quasi spherical objects followed by a size preserving operation retaining two largest round objects is performed. Slices between an axial slice located closely to centers of mass of the two detected round objects and top most slice mark a sub volume when IL and VS are searched (fig. 2). The PIL is found as a line perpendicular to the line connecting center of mass of the two spherical objects and projected on an axial slice of the sub volume (fig. 4a).

IL can be found by utilizing morphological processing of the T1 sub volume data and a rectangular region of interest found around the PIL. A width of the region of interest is dynamically adjusted and set to 15% of maximal horizontal width in HM2 mask (fig. 4b). Next, a morphological *bothat* operation [15], [14] performed on the analyzed cross-section with the superimposed mask, is computed (fig. 4b). This step is followed by morphological erosion of the region with a line-shape structuring element (fig. 4c). After thresholding of the image [10], pixels of the binary image (fig. 4c) are used to calculate IL coefficients by means of linear regression. A reader can note an angular variability between PIL (fig. 4d) and IL (fig. 4e) depicting differences in IL angle along axial slices.

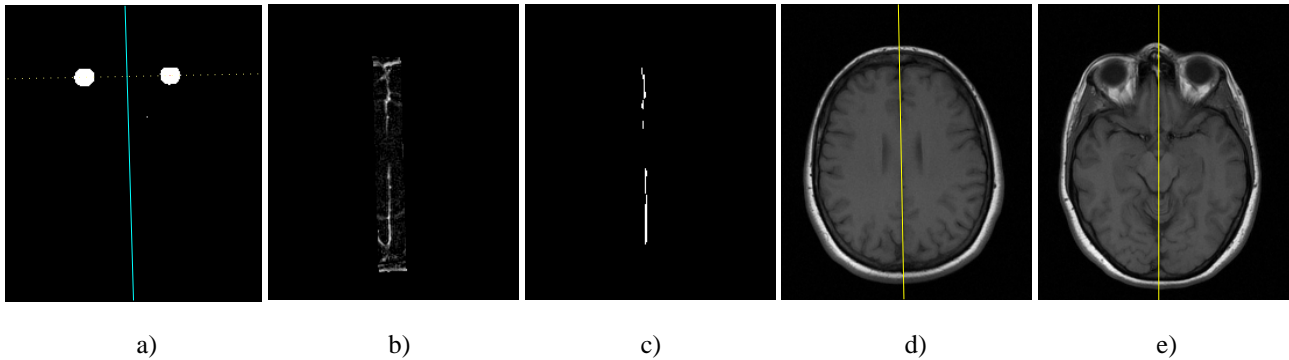


Figure 4. Example of interhemispheric line location: a) eyeballs detected in T2 series and PIL projected on a target slice (solid line), b) region of interest from T1 image after morphological *bothat* operation, c) binary image of b) with IL points within the region of interest d), e) examples of original T1 images with superimposed interhemispheric lines.

2.2.3 SEGMENTATION OF LATERAL VENTRICLES

Interhemispheric lines play a key role in the robust detection of the midsagittal plane and ventricular system segmentation from MR studies [12], [4]. In [3] a fast and robust algorithm of VS segmentation was described, however, the authors report that it works satisfactory when slice thickness is less than 3mm without gaps. Thus its usage in some clinical applications data may be limited. Hence a method of lateral ventricle segmentation from image data with thick slices has been developed. The human ventricular system consists of 4 ventricles: the two lateral, the third and the fourth, which communicate to form one interconnected structure [16]. The third and fourth ventricles are normally much smaller than the lateral ventricles, and thus the communication between them in thick slice MR studies with gaps may not be visible and difficult to model. Therefore our approach to segmentation of the VS is limited to segmentation of the LV. At this stage of the study it is assumed that if any part of the third and fourth ventricle is detected, then it is treated as an artifact.

The method starts with FCM segmentation [9] of 3D sub-volume data into 5 classes. Similar to [3] and [5], we model the presence of the following tissue classes: CSF, CSF-GM, GM, GM-WM and WM as an extension of the idea presented in fig. 3. As structures containing CSF, two classes (CSF, CSF-GM) with the lowest class center prototypes are selected. According to the 5-class model these two classes may contain GM voxels. Their number can be reduced by removal of pixels exceeding a certain threshold [5]. The threshold value was selected experimentally: $T_{CSF} = \text{mean}(CSF_{\text{pixels}}, CSF - GM_{\text{pixels}}) + 2\text{std}(CSF_{\text{pixels}}, CSF - GM_{\text{pixels}})$ where *mean* and *std* are mean value and standard deviation of gray level pixels respectively. In order to preserve CSF compartments located inside a sub-volume, a removal technique is applied to all CFS structures connected to the sub-volume borders. This helps to remove CSF compartments located in subarachnoid and sulcal spaces in the uppermost slices. The next step of the analysis is to find an axial cross-section (a marker slice) containing large parts of LV bodies. In this case, the thresholded sub-volume is scanned slice by slice downwards from the top by means of a LV mask. This mask consists of two rectangles evenly placed on left and right side of IL. Mask size was selected experimentally in testing data set. Due to discrepancies of LV shape and size in control and NPH subjects, the LV bodies are considered to be detected if they cover at least 8% of the mask area. If

such a slice is found, 3D connectivity between consecutive cross-sections upwards is checked and all 3D connected voxels are considered to be parts of LV. If no 3D connectivity occurs then the algorithm stops and cross-sections located below the marker slice are checked. Similar logic is applied while checking 3D connectivity downwards below the marker slice. In this case dilated by morphological operators leftmost and rightmost parts of detected LV bodies in consecutive slices are used for 3D connectivity checking. This prevents non ventricular voxels (in cisterns and sulcal CSF areas) from being appended to already extracted LV bodies. In last stage, volume of LV is calculated and 3D reconstruction of LV is displayed (fig. 5).

3. RESULTS

The algorithm was initially developed on 20 randomly selected cases from control group and 3 from NPH cases. This data set was used to adjust the threshold values, the size of structuring elements and the binary masks utilized by morphological operators in interhemispheric line detection and in 3D connectivity analysis in the lateral ventricular region. Based on segmentation results performed by the approach proposed in this paper, head masks, interhemispheric lines and lateral ventricles volumes were computed in a test group containing 4 NPH cases and 20 non NPH cases. Volume data measurements yielded lateral ventricular volumes of $12.5 \pm 4.1 \text{ ml}$ and $83.94 \pm 10.5 \text{ ml}$ in non-NPH subjects and NPH patients respectively.

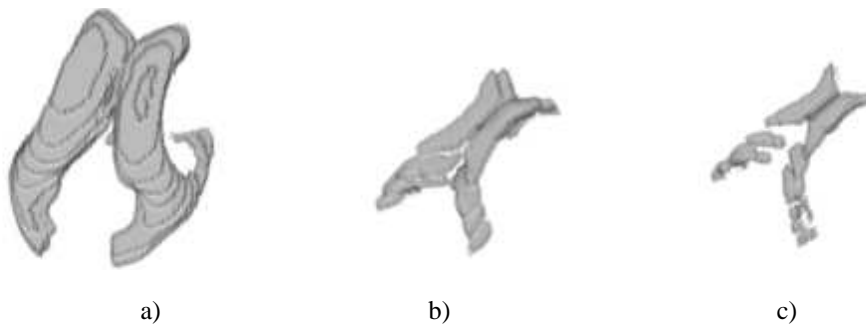


Figure 5. Results of 3D volume rendering of lateral ventricles segmented out by the proposed methodology: a) LV of a 68 year old male NPH patient, b) LV of a 54 year female old control patient, c) LV of a 31 male control patient.

4. CONCLUSION AND FUTURE WORK

A method for segmenting of lateral ventricles by prior location of interhemispheric lines from T1/T2 MR studies is proposed in this paper. Volumes of LV in NPH patients are bigger than those of control subjects. Results obtained in test studies and validated by a non-expert observer show good accuracy of the proposed approach. The algorithm correctly outlines central parts of the lateral ventricles in axial cross-sections and there was no leakage from cisternal and sulcal CSF compartments noted during methodology testing. However, in five control cases, some thinner parts of the frontal horns of the LV failed to segment due to poor contrast between GM and CSF areas, yielding false negative detection. This error was compounded in an additional three cases where missed parts of the posterior horns of the LV were located too far from the bodies of the LV, causing a segmentation discontinuity. The total volume of disconnected parts in single case did not exceed 7% of the remaining correctly segmented bodies of LV in the same case. Improvement of the

segmentation procedure and anatomical knowledge based approach to overcome these shortcomings will be considered. Validation of interhemispheric line location and segmentation results by a clinical expert will be addressed in future work. If satisfactory accuracy is achieved, the existing approach to the quantification of size and shape of ventricular system will be improved by the additional functionalities of: automated measurement of ventricular ballooning (shape quantification), measurement of the callosal angle formed by the frontal horns of lateral ventricles, volume measurement of the remaining CSF compartments as well as volume measurement of other intracranial structures. This may be useful in monitoring patient condition before and after shunt surgery. Better selection of shunt candidacy by improved characteristics may also be beneficial for NPH diagnosis and treatment.

BIBLIOGRAPHY

- [1] Meier U., Paris S., Grawe A., Stockheim D., Hajdukova A., Mutze S., Is there a correlation between operative results and change in ventricular volume after shunt placement? A study of 60 cases of idiopathic normal-pressure hydrocephalus. *Neuroradiology* (2003) 45: 377–380
- [2] Marmarou A., Bergsneider M., Klinge P., Relkin N., McL. Black P., The value of supplemental prognostic tests for the preoperative assessment of idiopathic normal-pressure hydrocephalus. Guidelines for the diagnosis and management of idiopathic normal pressure hydrocephalus. *Supplement to Neurosurgery Journal*, Vol. 57, No. 3, 2005, pp S2-1-S2-52
- [3] Xia Y., Quingmao H., Aziz A., Nowinski W., A knowledge-driven algorithm for a rapid and automatic extraction of the human cerebral ventricular system from MR neuroimages., *Neuroimage*, Vol., 21, pp. 269-282, 2004
- [4] Schnack H.G., Hulshoff Pol H.E., Baare W.F., Viergever M.A., Kahn R.S., Automatic segmentation of the ventricular system from MR images of the human brain, *Neuroimage*, Vol. 14, pp95-104, 2001
- [5] Lemieux L., Hammers A., Mackinnon T., Liu R., Automatic segmentation of the brain and intracranial cerebrospinal fluid in T1 weighted Volume MRI scans of the head and its application to serial Cerebral and Intracranial Volumetry, *Magnetic Resonance in Medicine*, Vol. 49, pp; 872-884, 2003
- [6] Clark M., Hall L., Goldgof D., Velthuisen R., Murtagh R., Silbiger M., Automatic tumor segmentation using knowledge-based techniques, *IEEE Trans on Medical Imaging*, Vol. 17, No 2, pp. 187-201, 1998
- [7] Vaidyanathan M., Clarke L., Heidtman C., Velthuisen R., Hall L., Normal brain volume measurements using multispectral MRI segmentation, *Magnetic Resonance Imaging*, Vol. 15, No. 1, pp. 87-97, 1997
- [8] Clark M., Hall L., Goldgof B., Clarke., Velthuisen R., Silbinger M., MRI segmentation using fuzzy clustering techniques, *IEEE Engineering in Medicine and Biology*, Vol. 13, No. 5., pp. 730-742, 1994
- [9] Bezdek J.C., Hall L.O., Clark L.P., Review of MR, Image Segmentation Techniques using Pattern Recognition, *Medical Physics*, V01.20, No. 4, 1993, pp.1033-1048.
- [10] Zack G.W., Rogers W.E., Latt S.A., Automatic measurement of sister chromatid exchange frequency, *J Histochem Cytochem*. 1977 vol. 25 (7):741-53.
- [11] Dempster A, Laird N, Rubin D. Maximum likelihood from incomplete data via the EM algorithm. *Journal of the Royal Statistical Society, Series B*, Vol. 39 no. pp:1–38, 1977
- [12] Quingmao H., Nowinski W., A rapid algorithm for robust and automatic extraction of the midsagittal plane of the human cerebrum from neuroimages based on local symmetry and outlier removal, *Neuroimage*, Vol. 20, pp. 2153-2165, 2003
- [13] Liu Y., Collins R, Rothfus W, Robust midsagittal plane extraction from normal and pathological 3D neuroradiology image. *IEEE Trans. Med Imag.* Vol. 20, no 3 pp. 173-192
- [14] Haralick, R. M., Shapiro L.G., *Computer and Robot Vision*, Volume I, Addison-Wesley, 1992, pp. 28-48.
- [15] Pratt, W.K., *Digital Image Processing*, John Wiley & Sons, Inc., 1991
- [16] Blatter D.D, Bigler E.D, Gale S.D, Johnson S.C, Anderson C.V, Burnett B.M, Parker N., Kurth S, Horn S.D, Quantitative Volumetric analysis of brain MR: normative database spanning 5 decades of life, *Am J Neuroradiol* 16:241–251, February 1995